

4-1999

## Magnetic Phase Diagrams of Erbium

B. H. Frazer

*Southern Illinois University Carbondale*

J. R. Gebhardt

*Southern Illinois University Carbondale*

N. Ali

*Southern Illinois University Carbondale*

Follow this and additional works at: [http://opensiuc.lib.siu.edu/phys\\_pubs](http://opensiuc.lib.siu.edu/phys_pubs)

© 1999 American Institute of Physics

Published in *Journal of Applied Physics*, Vol. 85 No. 8 (1999) at doi: [10.1063/1.370274](https://doi.org/10.1063/1.370274)

---

### Recommended Citation

Frazer, B. H., Gebhardt, J. R. and Ali, N.. "Magnetic Phase Diagrams of Erbium." (Apr 1999).

This Article is brought to you for free and open access by the Department of Physics at OpenSIUC. It has been accepted for inclusion in Publications by an authorized administrator of OpenSIUC. For more information, please contact [opensiuc@lib.siu.edu](mailto:opensiuc@lib.siu.edu).

## Magnetic phase diagrams of erbium

B. H. Frazer, J. R. Gebhardt, and N. Ali<sup>a)</sup>

*Department of Physics, Southern Illinois University at Carbondale, Carbondale, Illinois 62901 USA*

The magnetic phase diagrams of erbium in the magnetic field–temperature plane have been constructed for applied magnetic fields along the  $a$  and  $b$  axes. For an  $a$ -axis applied field our  $H$ – $T$  phase diagrams determined from magnetization and magnetoresistance data are in good agreement and consistent with that of Jehan *et al.* for temperatures below 50 K. A splitting of the basal plane Néel temperature ( $T_{N\perp}$ ) above 3.75 T introduces two new magnetic phases. Also a transition from a fan to a canted fan phase as suggested by Jehan *et al.* is observed in an increasing field below  $T_C$ . Our phase diagram for a  $b$ -axis applied field constructed from magnetization data is very similar to the phase diagram of Watson and Ali using magnetoresistance measurements. However, the anomaly at 42 K reported by Watson and Ali is not observed in the present study. No splitting of the  $T_{N\perp}$  transition is observed in either work for a field applied along the  $b$  axis. © 1999 American Institute of Physics. [S0021-8979(99)41308-8]

The complex magnetic structure of erbium has received much attention. The first neutron studies of erbium were performed by Cable *et al.*<sup>1</sup> and found three distinct ordering states in zero field. Below the longitudinal Néel temperature ( $T_{N\parallel}$ ) of  $\sim 87$  K, Er was found to order antiferromagnetically. Below the Curie temperature ( $T_C$ ) of approximately 19 K, erbium exhibits a conical structure with a ferromagnetic component along the  $c$  axis. Recently Gschneidner and Pecharsky<sup>2</sup> have observed both superheating and supercooling in ultrahigh purity erbium at the Curie temperature. They also report on the existence of several metastable intermediate phases between the ferromagnetic and antiferromagnetic structures. This suggests that impurities could have an important role in the magnetic structure of Er in this region. Between the longitudinal Néel ( $T_{N\parallel}$ ) and the basal plane Néel temperatures ( $T_{N\perp} \sim 52$  K) it is well known that erbium orders antiferromagnetically with a sinusoidal  $c$ -axis wave vector<sup>1,3</sup> and a modulation period of approximately seven layers.<sup>4</sup> Between  $T_{N\perp}$  and  $T_C$  mean field calculations have shown that a series of nonplanar cycloidal structures are energetically favored.<sup>3</sup> In this model the magnetic moments form an elliptical cycloid in the  $a$ – $c$  plane. A small  $b$ -axis component causes the moments to tilt out of the plane creating a structure known as a wobbly cycloid.<sup>5</sup> In this article we present the  $H$ – $T$  phase diagrams for applied magnetic fields along the  $a$  and  $b$  axes using magnetization and magnetoresistance measurements. Magnetic structures have been suggested using the results of Jehan *et al.*<sup>6</sup>

Two erbium single crystal samples prepared by the Ames Laboratory were used in this study. The first crystal has a  $b$ -axis length of 11.2 mm and cross section of  $1.1 \times 1.6$  mm<sup>2</sup> with a mass of 164 mg. The second crystal has an  $a$ -axis length of 10.5 mm and a cross section of  $1.0 \times 0.4$  mm<sup>2</sup> with a mass of 45 mg. Magnetization measurements were performed in a Quantum Design superconducting quantum interference device (SQUID) magnetometer.

Measurements as a function of temperature from 5 to 120 K in a constant applied magnetic field, and as a function of applied field from 0.01 to 5.5 T at a constant temperature were performed. Electrical resistance measurements were also performed on the  $a$ -axis crystal using the SQUID's magnetic field and temperature control systems. Employing the standard four probe method, a 32 mA longitudinal current was applied using a Keithley 220 current source and the voltage measured with a Keithley 181 nanovoltmeter. Resistance versus temperature measurements from 5 to 120 K at constant field and resistance versus field measurements from 0 to 4.0 T at constant temperature were performed. The samples were cooled in zero field and data were taken as the temperature was increased.

A large number of magnetization ( $M$ ) versus temperature ( $T$ ) scans have been carried out at constant applied magnetic fields ( $H$ ) along the  $a$  and  $b$  axes of Er. In addition, resistance ( $R$ ) versus temperature scans have been conducted for applied fields along the  $a$  axis. In Fig. 1(a) we present an  $M$  versus  $T$  curve for an applied field of  $H=0.1$  T along the  $b$  axis. Magnetic transitions are marked by arrows. Transitions are determined from step changes or slope changes in the data. The inset of Fig. 1(a) shows the slope of  $M$  versus  $T$ . This can be used to determine small slope changes in the data. The reason for using the derivative becomes clear in Fig. 1(b) where an  $R$  versus  $T$  curve is shown. Some of the magnetic transitions (indicated by arrows) are difficult to see in the original data but are clearly visible in the slope of  $R$  versus  $T$  given in the inset. Peaks not marked as magnetic transitions are determined to be noise due to their inconsistent appearance in  $dR/dT$  versus  $T$  curves at different applied fields.

In Figs. 2(a) and 2(b) several  $M$  versus  $H$  and  $R$  versus  $H$  curves for fields applied along the  $a$  axis are presented. Magnetic transition fields are again determined by step changes or slope changes in the data. By tabulating the transition temperatures at a given field and the transition fields at a given temperature, we are able to construct an  $H$ – $T$  phase diagram of Er. The transition indicated by arrows in Fig. 2

<sup>a)</sup> Author to whom correspondence should be addressed; electronic mail: nali@physics.siu.edu

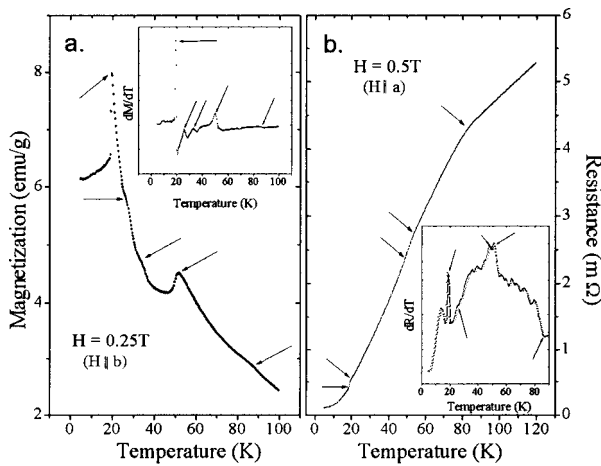


FIG. 1. (a) Magnetization vs temperature for a magnetic field of  $H = 0.25$  T applied along the  $b$  axis. The inset shows the derivative of the curve. Arrows indicate magnetic transitions. (b) Resistance vs temperature for an  $a$ -axis applied field of  $H = 0.5$  T. The derivative of the curve is shown in the inset. Arrows indicate magnetic transitions.

corresponds to the transition from the ferromagnetic fan phase to the canted ferromagnetic phase suggested by Jehan *et al.*<sup>6</sup> (Fig. 5). This transition is indicated by arrows in Fig. 3 where we present the  $H-T$  phase diagram of Er for applied fields along the  $a$  axis.

Figure 3(a) shows the phase diagram determined from magnetization data and Fig. 3(b) is the phase diagram determined by magnetoresistance measurements. The two phase diagrams are very similar showing a Curie temperature of  $T_C = 19$  K, a basal plane Néel temperature of  $T_{N\perp} = 52$  K and a longitudinal Néel temperature of  $T_{N\parallel} = 87$  K. Using thermal expansion measurements, these transitions have been shown by Watson and Ali<sup>7</sup> to be of first order, weak first order, and second order, respectively. In addition, zero field anomalies at  $T = 26, 34,$  and  $50$  K are observed. Our phase diagrams at low temperatures also agree well with that of Jehan *et al.*<sup>6</sup> whose results have been used to label regions of our phase

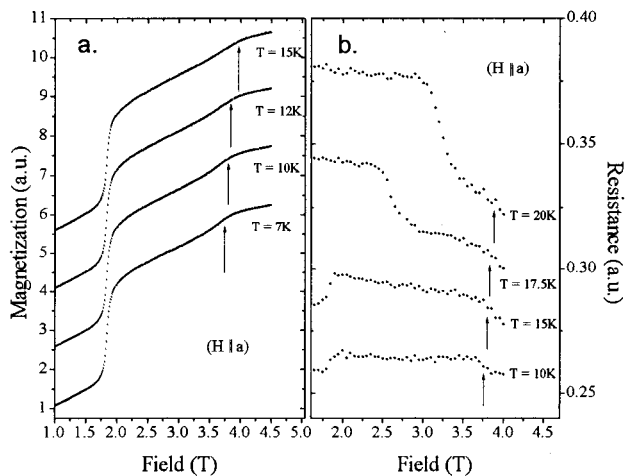


FIG. 2. (a) Magnetization vs field and (b) resistance vs field for  $(H \parallel a)$ . The arrows indicate the transition from a ferromagnetic fan to a canted ferromagnetic fan phase suggested by Jehan *et al.* (Ref. 6). For clarity, all curves have been offset along the vertical.

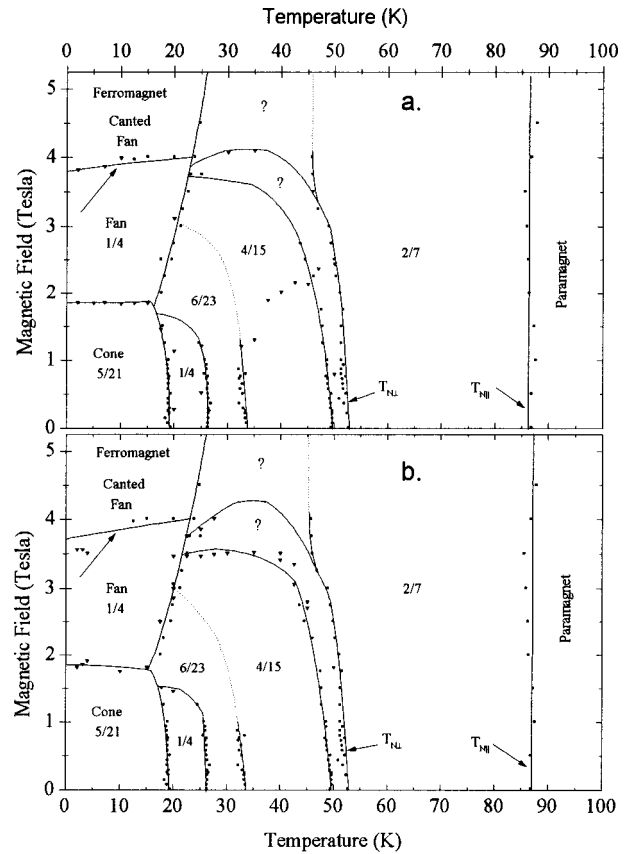


FIG. 3.  $H-T$  phase diagrams of single-crystal erbium for applied magnetic field along the  $a$  axis constructed from (a) magnetization measurements and (b) magnetoresistance measurements. Square symbols (■) indicate temperature dependent data and triangular symbols (▼) represent field dependent data. Lines are a visual guide.

diagrams. One exception is a series of anomalies beginning at  $34$  K and  $1$  T, and ending at around  $45$  K and  $2.25$  T. These anomalies are not observed in magnetoresistance data [Fig. 3(b)] and are possibly due to an incommensurate phase. The transition at  $34$  K is not observed above  $1.25$  T; however, we believe this transition shifts to lower temperatures as the field increases forming the upper boundary of the commensurate  $(6/23)$  cycloidal structure. This is indicated by a dashed line in Fig. 3. A second commensurate structure with a wave vector of  $\mathbf{q}_c = (4/15)\mathbf{c}^*$  is bounded by the  $50$  K transition which shifts towards lower temperatures above  $3$  T. A splitting of the  $T_{N\perp}$  transition above  $3.5$  T is observed with one feature shifting to lower temperatures and the other remaining at a constant temperature in an increasing field. This latter feature was observed by Jehan *et al.*<sup>6</sup> as weak peaks in the neutron scattering data. This splitting of  $T_{N\perp}$  forms two regions which separate the  $(4/15)$  cycloidal and  $(2/7)$  modulated structures and do not correspond to any previously reported phases. However, Jehan *et al.*<sup>6</sup> does suggest the possibility of a helifan-like structure in this region. The longitudinal Néel temperature ( $T_{N\parallel}$ ) is observed to be independent of temperature in an increasing field.

In Figure 4(a) we present the  $H-T$  phase diagram of Er for an applied magnetic field along the  $b$  axis determined from magnetization data. Anomalies at  $T_C = 19$  K,  $T_{N\perp} = 52$  K, and  $T_{N\parallel} = 87$  K as well as transitions at  $T = 32$  and

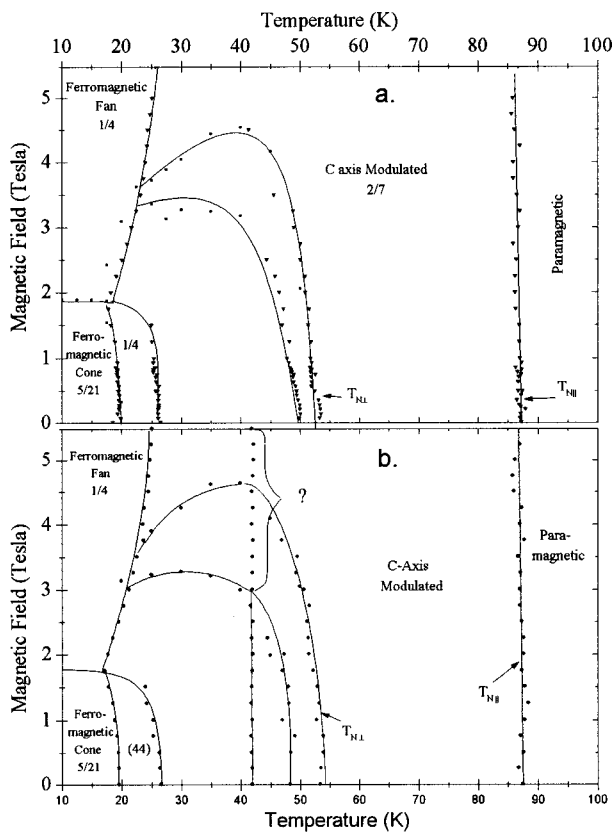


FIG. 4. (a)  $H$ - $T$  phase diagram of single-crystal erbium for applied magnetic field along the  $b$  axis constructed from magnetization measurements. Square symbols ( $\blacksquare$ ) indicate  $M$  vs  $T$  data and triangular symbols ( $\blacktriangledown$ ) represent  $M$  vs  $H$  data. Lines are a visual guide. (b)  $H$ - $T$  phase diagram ( $H\parallel b$ ) of Watson and Ali (Refs. 7 and 9) using magnetoresistance data.

50 K are observed. The phase diagram agrees quite well with the work of Watson and Ali,<sup>8,9</sup> whose phase diagram produced from magnetoresistance data is given in Fig. 4(b). Corresponding magnetic structures are labeled using the results of Watson and Ali.<sup>6,8,9</sup> At low temperatures a transition from a ferromagnetic cone to a ferromagnetic fan phase is observed just below 2 T. A transition from the fan phase to a series of antiferromagnetic structures is seen above  $H=2$  T and shifts towards higher temperatures at larger fields. A transition at 32 K is seen to change little with temperature

until 1 T when it shifts towards lower temperatures, and eventually merges with the  $T_C$  transition at about 1.5 T. An anomaly at 50 K is seen to shift slightly towards lower temperatures in an increasing field until 2.5 T when this shift becomes more pronounced and the anomaly intersects the fan transition at around 3.5 T. The  $T_{N\perp}$  transition is observed shifting to lower temperatures in an increasing field until 4.5 T when the shift towards lower temperatures continues in a decreasing field and merges with the fan line at about 3.75 T. The  $T_{N\parallel}$  transition remains at a constant temperature in an increasing field. The  $b$ -axis phase diagram is very similar to the  $a$ -axis phase diagram at low temperatures. Also a similar region between the 50 K and the  $T_{N\perp}$  transitions is observed. However, no splitting of  $T_{N\perp}$  is observed for fields applied along the  $b$  axis.

We have constructed the  $H$ - $T$  phase diagrams of Er for applied magnetic fields along the  $a$  and  $b$  axes. At temperatures below 50 K our  $a$ -axis phase diagram agrees well with that of Jehan *et al.*<sup>6</sup> A transition from a fan to a canted fan phase as suggested by Jehan *et al.*<sup>6</sup> is observed at 4 T and a splitting of  $T_{N\perp}$  above 3.5 T as well as two previously unobserved phases separating the (4/15) and (2/7) commensurate phases are presented. The magnetic structure of these new regions needs to be determined by neutron diffraction experiments. Our  $b$ -axis phase diagram agrees well with the phase diagram of Watson and Ali.<sup>8,9</sup>

This work was supported in part by a grant from the Consortium for Advanced Radiation Source, University of Chicago, Chicago, Illinois.

- <sup>1</sup>J. W. Cable, E. O. Wollan, W. C. Koehler, and M. K. Wilkinson, *Phys. Rev.* **140**, 1896 (1965).
- <sup>2</sup>K. A. Gschneidner Jr. and V. K. Pecharsky, *Phys. Rev. Lett.* **78**, 4281 (1997).
- <sup>3</sup>R. A. Cowley and J. Jensen, *J. Phys.* **4**, 9673 (1992).
- <sup>4</sup>J. Jensen and R. A. Cowley, *Europhys. Lett.* **21**, 705 (1993).
- <sup>5</sup>M. K. Sanyal, D. Gibbs, J. Bohr, and M. Wulf, *Phys. Rev.* **49**, 1079 (1994).
- <sup>6</sup>D. A. Jehan, D. F. McMorrow, J. A. Simpson, R. A. Cowley, P. P. Swadling, and K. N. Clausen, *Phys. Rev.* **50**, 3085 (1994).
- <sup>7</sup>B. Watson and N. Ali, *J. Phys.* **7**, 4713 (1995).
- <sup>8</sup>B. Watson and N. Ali, *J. Phys.* **8**, 1797 (1996).
- <sup>9</sup>B. Watson and N. Ali, *J. Alloys Compd.* **250**, 662 (1997).